How to cite: *Angew. Chem. Int. Ed.* **2024**, *63*, e202411105
doi.org/10.1002/anie.202411105

Protein Modifications

Red-Shifting B_{12}-Dependent Photoreceptor Protein via Optical Coupling for Inducible Living Materials

Hong Kiu Francis Fok, Z. Yang, Xin Dai, Qikun Yi, Chi Ming Che, Lingxiang Jiang, Liting Duan, Jinqing Huang, Zhongguang Yang,* and Fei Sun**

Abstract: Cobalamin (B_{12})-dependent photoreceptors are gaining traction in materials synthetic biology, especially for optically controlling cell-to-cell adhesion in living materials. However, these proteins are mostly responsive to green light, limiting their deep-tissue applications. Here, we present a general strategy for shifting photoresponse of B_{12}-dependent photoreceptor $CarH_C$ from green to red/far-red light via optical coupling. Using thiol-maleimide click chemistry, we labeled cysteine-containing $CarH_C$ mutants with SulfoCyanine5 (Cy5), a red light-capturing fluorophore. The resulting photoreceptors not only retained the ability to tetramerize in the presence of adenosylcobalamin ($AdoB_{12}$), but also gained sensitivity to red light; labeled tetramers disassembled on red light exposure. Using genetically encoded click chemistry, we assembled the red-shifted proteins into hydrogels that degraded rapidly in response to red light. Furthermore, *Saccharomyces cerevisiae* cells were genetically engineered to display $CarH_C$ variants, which, alongside in situ Cy5 labeling, led to living materials that could assemble and disassemble in response to $AdoB_{12}$ and red light, respectively. These results illustrate the $CarH_C$ spectrally tuned by optical coupling as a versatile motif for dynamically controlling cell-to-cell interactions within engineered living materials. Given their prevalence and ecological diversity in nature, this spectral tuning method will expand the use of B_{12}-dependent photoreceptors in optogenetics and living materials.

Introduction

Naturally occurring photoresponsive proteins such as rhodopsins,[1] light-harvesting chlorophyll-binding proteins,[2] and light-oxygen-voltage-sensing domains (LOV), cryptochrome 2 proteins (Cry2),[3] play crucial roles in vision, photosynthesis, and metabolic regulation. Their photophysical properties are governed largely by their respective cofactors (i.e., retinals, chlorophylls, and flavins) and, to less extent, by the amino acid residues surrounding these cofactors. However, these small-molecule chromophores are inherently limited in spectral range by their chemical structures; the motifs such as retinals and flavins are predominantly blue light-responsive, despite their pivotal roles in optogenetics.[3–4] Although it has proven feasible to spectrally tune these optogenetic tools via protein engineer-

[*] H. K. F. Fok, Dr. Q. Yi, Dr. Z. Yang, Prof. Dr. F. Sun
Department of Chemical and Biological Engineering
The Hong Kong University of Science and Technology
Clear Water Bay, Kowloon, Hong Kong SAR, 999077, China
E-mail: zyangal@connect.ust.hk
kefsun@ust.hk

Dr. X. Dai, Prof. Dr. J. Huang
Department of Chemistry
The Hong Kong University of Science and Technology
Clear Water Bay, Kowloon, Hong Kong SAR, 999077, China

Dr. X. Dai, Prof. Dr. C. M. Che
Laboratory for Synthetic Chemistry and Chemical Biology
Health@InnoHK
Hong Kong Science Park, New Territories, Hong Kong SAR, 999077, China

Prof. Dr. L. Jiang
South China Advanced Institute for Soft Matter Science and Technology
School of Emergent Soft Matter, South China University of Technology
Guangzhou 510640, China

Prof. Dr. L. Duan
Department of Biomedical Engineering
The Chinese University of Hong Kong
Sha Tin, Hong Kong SAR, 999077, China

Prof. Dr. F. Sun
Greater Bay Biomedical InnoCenter
Shenzhen Bay Laboratory
Shenzhen 518036, China

Prof. Dr. F. Sun
Biomedical Research Institute
Shenzhen Peking University—The Hong Kong University of Science and Technology Medical Center
Shenzhen 518036, China

Prof. Dr. F. Sun
Research Institute of Tsinghua
Pearl River Delta
Guangzhou 510530, China

Dr. Z. Yang
Center for Engineering Materials and Reliability
Fok Ying Tung Research Institute, The Hong Kong University of Science and Technology (Guangzhou)
Guangzhou, China
E-mail: zyangal@connect.ust.hk

ing strategies like directed evolution, these processes often entail laborious trial-and-error efforts,[5] and lead to solutions that are not generalizable and can hardly be transferred from one system to the other.

Cobalamin (B_{12})-based photoreceptor proteins have garnered significant attention in recent years.[5b,6] For instance, *Thermus thermophilus* CarH, a bacterial transcriptional regulator involved in carotenoid biosynthesis, modulates gene expression in response to light (Figure 1A). Specifically, its C-terminal B_{12}-binding domain ($CarH_C$) tetramerizes upon binding to adenosylcobalamin ($AdoB_{12}$, K_d of ~0.8 μM), thus activating the DNA-binding of the N-terminal domains.[7] On light exposure (<570 nm), the tetramers disassemble into monomers, accompanied with the cleavage of the C–Co bond between the upper 5′-deoxyadenosyl ligand and the cobalt center, the formation of bis-His-ligated B_{12}, and the dissociation of proteins from DNA. The unique properties of $CarH_C$ have enabled the creation of various smart biomaterials and optogenetic tools.[8] The C–Co bond in $AdoB_{12}$ is particularly sensitive to green light (~522 nm). For deep-tissue applications, it is highly desirable to make these B_{12}-dependent photoreceptor proteins responsive to red/far-red light. To this end, an obvious way is to use cofactor engineering, as $AdoB_{12}$ has previously been chemically modified to gain sensitivity toward red/far-red light via optical coupling.[9] The fluorophores such as SulfoCyanine5 (Cy5), Atto725, and DyLight800 appended to its ribose 5′-OH act as antennas to capture red/far-red light (up to 800 nm) and promote cleavage of the C–Co bond, likely via contact quenching between the light-capturing antenna and the corrin ring of B_{12}.[9] However, despite its proved feasibility and seeming straightforwardness, we should never underestimate the difficulty in modifying these complex B_{12} molecules, of which the total synthesis is still touted as a monumental achievement of the century.[10] Besides, the conjugation of

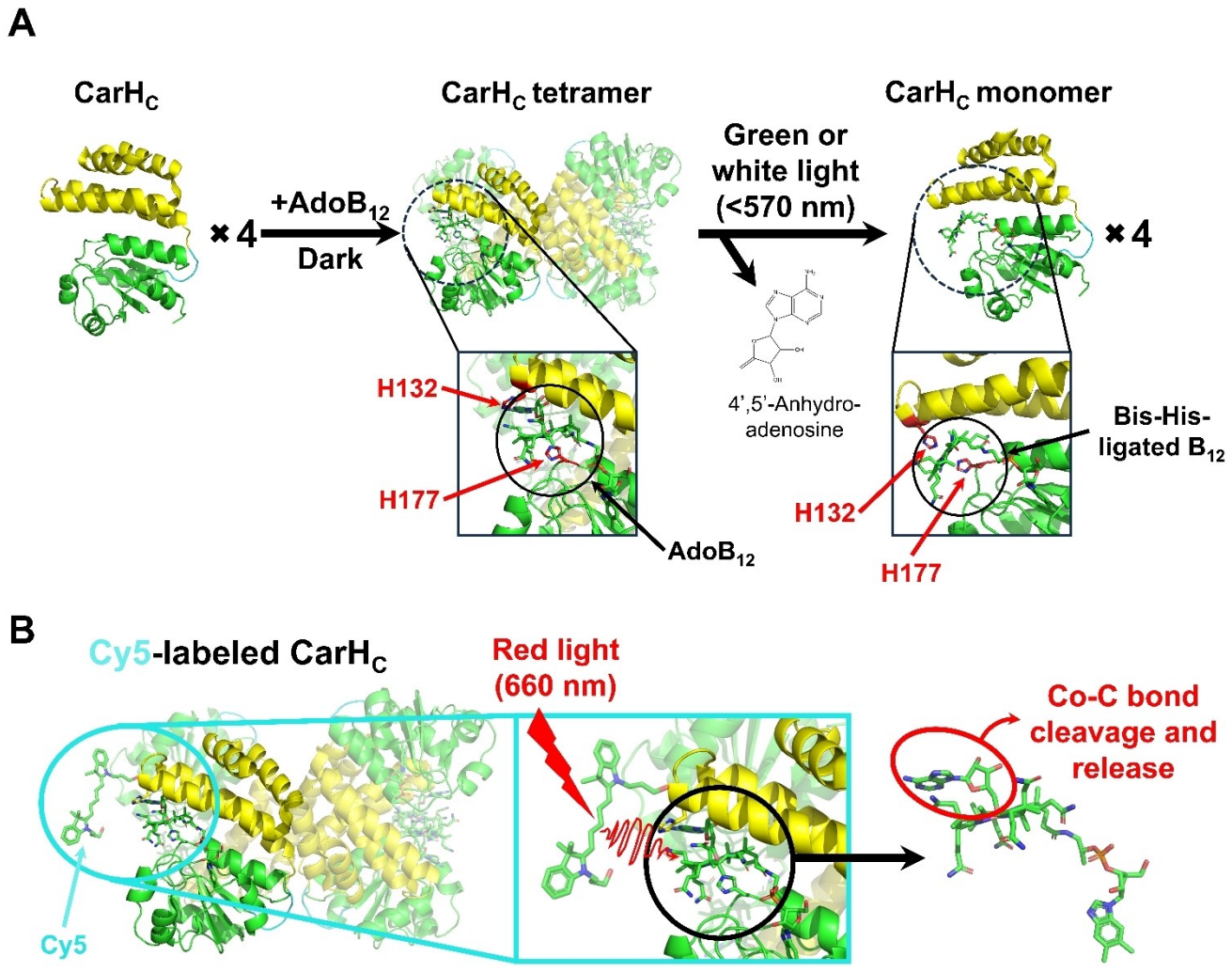

Figure 1. Photochemistry of $CarH_C$. (A) $AdoB_{12}$ induces tetramerization of $CarH_C$, while photolysis of $AdoB_{12}$ triggers the disassembly of the tetramer, accompanied with the release of 4′,5′-anhydroadenosine and the formation of bis-His-ligated B_{12}. The N-terminal four-helix bundle, the unstructured loop region, and the C-terminal Rossmann-fold domain are highlighted in yellow, cyan, and green, respectively. (B) Labeling $CarH_C$ with Cy5 via thiol-maleimide click chemistry red-shifts the photoresponse of the protein. The fluorophore Cy5 appended to the protein acts as an antenna to capture red light (~660 nm) and transfer energy to the corrin ring, thus facilitating the cleavage of the C–Co bond.

the ribose ring with a bulky fluorophore may perturb the protein-cofactor interaction, thus necessitating additional protein engineering efforts to restore it. To avoid these complications, a more facile and general approach to the spectral tuning of $CarH_C$ is needed.

Contact quenching between the fluorophore and the corrin ring has been proposed as a possible mechanism by which red/far-red light cleaves the C–Co bond in the $AdoB_{12}$ derivatives mentioned above. Unlike Förster resonance energy transfer, which requires both spatial proximity and wavelength overlap between the fluorophore and the quencher, the contact quenching-based optical coupling appears to require spatial proximity only.[9] In the case of B_{12}-binding proteins, other than directly conjugating the fluorophore with $AdoB_{12}$ to achieve such proximity, an alternative way is to leverage the protein scaffolds (Figure 1B). Indeed, nature has already adopted this strategy for generating red/far-red light-responsive photoreceptor proteins;[6a,11] a recent study revealed that photocobilins, a collection of naturally occurring, multi-center photoreceptor proteins, bind to B_{12} and the far-red light-capturing biliverdin simultaneously, between which the proximity leads to optical coupling and facile photolysis of $AdoB_{12}$ in response to far-red light.[12] We envisioned that $CarH_C$ could be red-shifted in a similar manner by decorating the protein scaffold with a red/far-red light-capturing chromophore, the latter of which would optically couple with $AdoB_{12}$ and facilitate its cleavage under red/far-red light. In this vein, we created several cysteine-containing $CarH_C$ mutants through site-directed mutagenesis. These mutants maintained their physiochemical properties after being labeled in situ with the fluorophore, Cy5-maleimide (Cy5-MAL), through thiol-maleimide click chemistry. Following $AdoB_{12}$-induced tetramerization, these tetramers became sensitive to red light and disassembled on red-light exposure, accompanied with C–Co scission. These red-shifted photoreceptors not only enabled the synthesis of red light-responsive protein hydrogels, but also dynamic assembly/disassembly of living cells in a red light-dependent manner. Thanks to its simplicity and modularity, spectrally tuning B_{12}-dependent photoreceptors via in situ fluorescent labeling will expand their use in materials science and optogenetics.

Results and Discussion

Fluorescent Labeling of $CarH_C$

$CarH_C$ is composed of an N-terminal four-helix bundle and a C-terminal Rossmann-fold domain, connected by a Gly- and Pro-rich unstructured loop. The cofactor $AdoB_{12}$ is sandwiched between the N- and C-terminal domains. To achieve contact quenching within this protein scaffold, we selected three representative sites for mutations (i.e., G134C, Ins164C, and A231C) and subsequent fluorescent labeling. These three sites were selected for their representation in the three domains of the protein: the N-terminal domain, loop region, and C-terminal domain, with varying orientations and distances (15.8, 35.9, and 16.3 Å) from $AdoB_{12}$. This selection enables us to investigate the potential impact of structural factors such as orientation and distance on contact quenching (Figure 2A). Besides, none of these sites are directly involved in $AdoB_{12}$ binding and protein tetramerization, thus minimizing the potential disruption caused by the mutations and fluorescent labeling on protein behavior.

We employed Cy5-MAL (maximum absorbance at 646 nm), a fluorophore that has proven safe and biocompatible in various biological applications,[13] to label the cysteine-containing mutants via thiol-maleimide Michael addition. UV/Vis spectroscopic analyses of the three mutants showed different labeling efficiencies: $76\pm2\,\%$ of $CarH_C$-G134C, $48\pm4\,\%$ of $CarH_C$-Ins164C, and $68\pm1\,\%$ of $CarH_C$-A231C were successfully conjugated with Cy5 (Figure S1). As the thiol-maleimide reaction often suffers from the competing thiol oxidation, the varying labeling efficiency may be caused by differences in the resistance to oxidation at these sites. Analyses by matrix-assisted laser desorption ionization–time of flight mass spectrometry (MALDI-TOF MS) confirmed the successful labeling of these protein mutants, $CarH_C$-G134C, $CarH_C$-Ins164C, and $CarH_C$-A231C, by Cy5-MAL (Figure S2). UV/Vis absorbance spectra of the three mutants after labeling revealed a peak at ~646 nm, corresponding to the maximum absorbance of Cy5, which further corroborates the formation of Cy5-protein conjugates (Figure S3).

We evaluated the long-term stability of the Cy5-protein conjugates under ambient conditions. Two or four days after storage at room temperature, the samples were centrifuged using centrifuge tube filters to remove unbound Cy5. Subsequently, UV/Vis spectroscopy was conducted to determine the Cy5 to protein ratio. Some loss of Cy5 was observed, while the majority remained intact; after two days at room temperature, $50\pm5\,\%$, $65\pm13\,\%$, and $68\pm6\,\%$ of Cy5-labeled G134C, Ins164C, A231C, respectively (Figure S4). The loss of Cy5 from the conjugates is likely caused by reversible Michael addition, which is common for thiol-maleimide conjugates.[14] Throughout the study, to minimize the effect of such degradation, most Cy5-protein conjugates were freshly prepared at a low temperature (4 °C) and used immediately after labeling.

Red Light-Induced Protein Disassembly

We subsequently examined the influence of fluorescent labeling on $CarH_C$ oligomerization and photoresponse using UV/Vis spectroscopy and native polyacrylamide gel electrophoresis (PAGE). The fusion protein, SpyTag-ELP-$CarH_C$ (AEC), and its cysteine-containing mutants, AEC-G134C, AEC-Ins164C, and AEC-A231C, were tested, as the ELP-fusion constructs were used mostly in the subsequent experiments. The UV/Vis spectral analysis revealed that both Cy5-AEC-G134C and Cy5-AEC-A231C, but not Cy5-AEC-Ins164C, gained heightened sensitivity to red light, even at low intensity ($0.01\,mW/cm^2$) (Figure 2B). The heightened sensitivity to red light was comparable to their green light sensitivity ($0.01\,mW/cm^2$) (Figures S5 and S6). The emer-

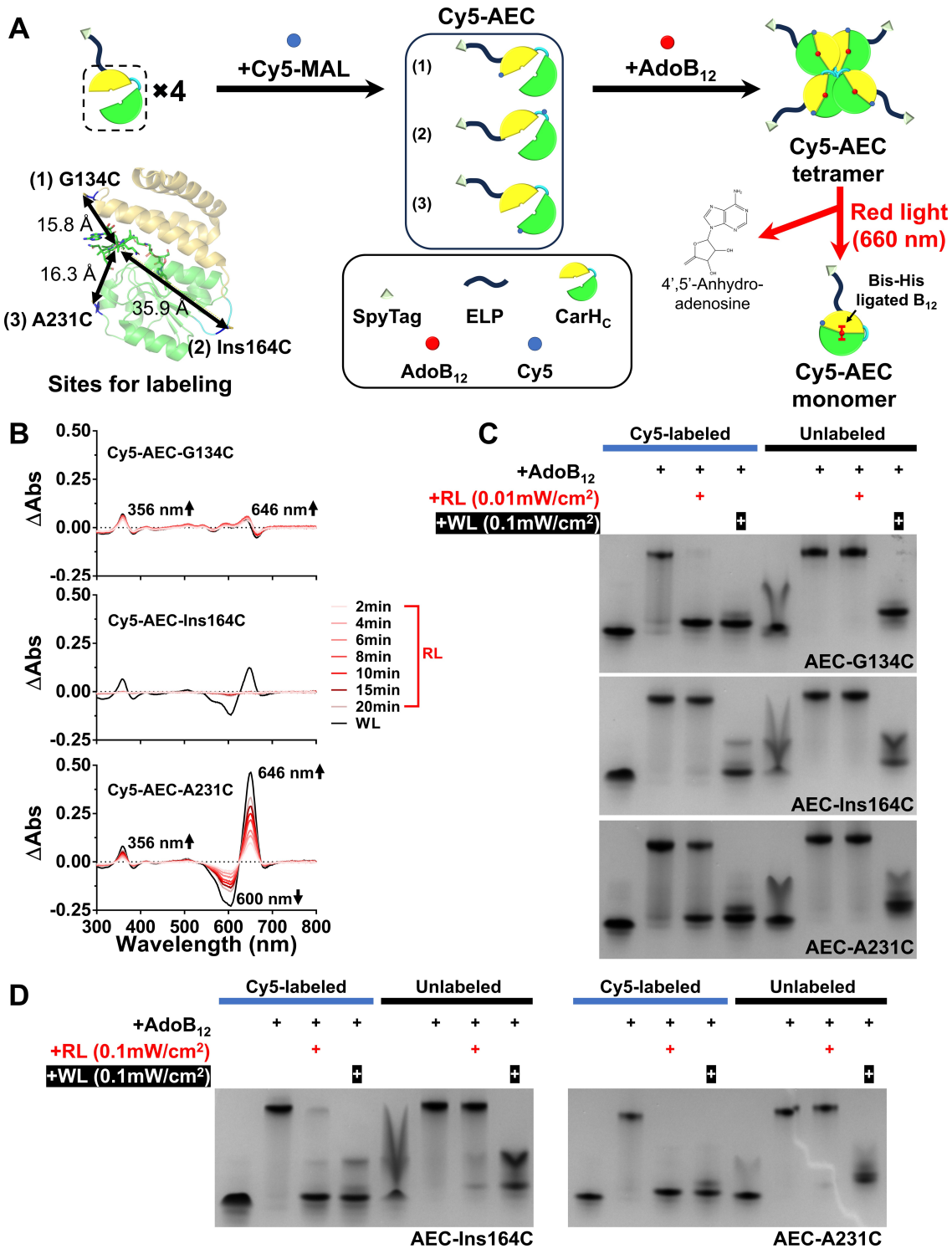

Figure 2. Cy5 labeling red-shifts SpyTag-ELP-CarH$_C$ (AEC). (A) Schematic showing photochemistry of Cy5-AEC. Distances between the possible Cy5-labeling sites (G134C, Ins164C, and A231C) and the Co center of AdoB$_{12}$ are shown. The cysteine-containing CarH$_C$ domain is labeled with Cy5 via thiol-maleimide Michael addition. The resulting Cy5-AEC retains its ability to bind to AdoB$_{12}$ and subsequently tetramerize. Exposure to red light disassembles AEC tetramers into monomers, accompanied with photolysis of AdoB$_{12}$ and formation of bis-His-ligated B$_{12}$. (B) Difference absorbance spectra of AdoB$_{12}$ bound Cy5-AEC variants after varied durations of illumination of red light (RL) (660 nm, 0.01 mW/cm^2) or white light (WL) (0.1 mW/cm^2). (C) Native PAGE analysis of AdoB$_{12}$-induced tetramerization and red light-induced disassembly of the three AEC variants, G134C, Ins164C, and A231C, with and without Cy5 labeling. Red light (RL) (660 nm, 5 min, 0.01 mW/cm^2). White light (WL) (10 min, 0.1 mW/cm^2). (D) Native PAGE analysis of AdoB$_{12}$-induced tetramerization and red light-induced disassembly of AEC-Ins164C and AEC-A231C, with and without Cy5 labeling, using stronger intensity of red light. Red light (RL) (660 nm, 5 min, 0.1 mW/cm^2). White light (WL) (10 min, 0.1 mW/cm^2).

gence of a peak at 356 nm upon red light exposure indicates the formation of photolyzed B_{12} product (Figure 2B). Interestingly, Cy5-AEC-Ins164C only responded to green light, not red light, indicating that the remoteness of this labeling site hindered the optical coupling between Cy5 and $AdoB_{12}$. Cy5 labeling was essential for the observed red-light sensitivity, as the unlabeled proteins failed to display spectral changes under red light (Figure S7).

Emission spectra further revealed that the binding of native $AdoB_{12}$ to proteins quenched the emission of Cy5 at 664 nm, suggesting effective optical coupling (Figure S8).[9,15] According to native PAGE, it turned out that the Cy5-labeled AEC variants all retained their abilities to tetramerize upon addition of $AdoB_{12}$, while gaining varied levels of red light-response, depending on the labeling sites. The native PAGE analyses showed that Cy5-AEC-G134C was still able to oligomerize in the presence of $AdoB_{12}$ (1 *eq.*). The densitometric analysis of the native PAGE results revealed that a substantial portion of Cy5-labeled tetramers (~88 %) disassembled on exposure to red light at a moderate intensity (0.01 mW/cm^2), in contrast to the unlabeled AEC-G134C tetramers, with negligible disassembly (~0 %) after red light illumination (Figure 2C and S9). This result suggests that Cy5 labeling at Cys134 is pivotal for the observed red light-induced protein disassembly. To rule out the possibility that Cy5-MAL might interfere the protein's photoresponse via nonspecific interaction, we treated wild-type $CarH_C$, free of Cys, with Cy5-MAL and observed no difference from the protein alone in their photoresponse (Figure S10); the tetramers induced by $AdoB_{12}$, with or without Cy5-MAL, largely remained under red light. This result suggests that specific covalent labeling is essential for optical coupling to occur.

It occurred to us that the efficiency of optical coupling was affected by the distance between the fluorophore and $AdoB_{12}$. In the case of Cy5-AEC-Ins164C, where the labeling site, Cys164, resides in the loop region and is more distant (35.9 Å) from the Co center than the N-terminal Cys134 is (15.8 Å), the tetramers turned out to be less sensitive to red light, which remained largely intact (> 90 %) after a moderate red-light exposure (0.01 mW/cm^2) and disassembled by ~90 % only after being exposed to stronger red light (0.1 mW/cm^2) (Figures 2C, 2D, S11 and S12). In addition to distance, other structural parameters might also affect optical coupling. Despite the fact that the C-terminal Cys231 is situated 16.3 Å away from the Co center, comparable to the N-terminal Cys134 (15.8 Å) in distance, the corresponding Cy5-AEC-A231C tetramers proved to be somewhat less sensitive to red light; only ~38 % of the tetramers disintegrated after red light exposure (0.01 mW/cm^2), substantially lower than Cy5-AEC-G134C (~90 %) (Figure 2C, S9 and S13 A). A careful inspection of the protein structure unveiled that the C-terminal Cys231 is on the *trans* side of the corrin ring, distal to the axial C–Co bond, while the N-terminal Cys134 resides on the *cis* side of the corrin, in proximity to the C–Co bond. This spatial arrangement might account for the distinct efficiency in optical coupling, although the exact mechanism for this has yet to be elucidated. Nevertheless, increasing red light intensity from 0.01 to 0.1 mW/cm^2 enhanced the disassembly of Cy5-AEC-A231C tetramers (~98 %) (Figure 2D and S13B), mirroring the behavior observed in Cy5-AEC-Ins164C. This highlights the effectiveness and robustness of this optical coupling strategy, regardless of the specific labeling sites.

We also examined the labeling with Cy7.5-MAL, a different fluorophore that is excited by near-infared light (788 nm). About 58 % of CarHC-Ins164C was successfully labeled by Cy7.5-MAL, comparable to that by Cy5-MAL, as determined by UV/Vis spectral analysis (Figure S14A) and confirmed by MALDI-TOF MS analysis (Figure S14B). The ensuing native PAGE analyses showed that only about 25 % of Cy7.5-labeled $CarH_C$-Ins164C tetramers disassembled under strong near-infrared light (780 nm, 1.5 mW/cm^2) (Figure S14C), while up to 69 % of Cy5-labeled tetramers disassembled under much milder red light (660 nm, 0.1 mW/cm^2) (Figure S11B). These findings suggest that Cy5 is more efficient in optically coupling with $AdoB_{12}$ than Cy7.5, probably because of a larger overlap between the emission and absorption wavelengths of Cy5 and $AdoB_{12}$.

Taken together, these results confirmed that the Cy5 fluorophore, when covalently appended to the $CarH_C$ protein scaffold at a judiciously chosen site, can serve as an effective antenna to capture red light, which further facilitates the photolysis of $AdoB_{12}$, and the disassembly of protein tetramers.

To further explore the potential advantages of controlling these systems with red light, we investigated the response of Cy5-AEC-G134C to red light in challenging deep tissue scenarios. A piece of 12-mm-thick pork meat was used to simulate a deep tissue environment. The Cy5-AEC-G134C and AEC-G134C solutions were mixed with $AdoB_{12}$ and incubated in the dark for at least 30 minutes at room temperature. The mixtures were then subjected to four conditions: (1) kept in the dark; (2) placed under pork meat and exposed to red light (660-nm LED, 0.2 mW/cm^2) for 5 minutes; (3) placed under pork meat and exposed to green light (520-nm LED, 0.2 mW/cm^2) for 5 minutes; (4) exposed to white light (Warsun®, 0.1 mW/cm^2) for 10 minutes. Analyses using native PAGE and subsequent densitometry revealed that approximately 95 % of Cy5-labeled tetramers disassembled upon exposure to red light, substantially higher than that exposed to green light (~40 %), which can be attributed to the deeper penetration of red light into biological tissues. In contrast, the unlabeled AEC-G134C tetramers showed minimal disassembly after illumination with red light and green light (< 10 %). These results highlight the advantage of using the red light-responsive $CarH_C$ variant enabled by Cy5 labeling in a deep-tissue environment.

Notably, Cy5-labeling, while conveying the additional red light-sensitivity, has largely preserved the original green light sensitivity of the proteins (Figure 2C, S5–S6 and S9–S15) and may have slightly increased it (Figure S15). The Cy5-labeled $CarH_C$ variants fully disassembled into monomers under white or green light, comparable to the unlabeled counterparts (Figure 2C and Figures S9–S15). The observed sensitization of Cy5-labeled proteins to green light

(Figure S15) may be due to the Cy5 fluorophore absorbing light in the 500–700 nm range, covering the green light spectrum, despite its maximum absorbance at 646 nm (Figure S3).

Red Light-Induced Protein Release from Hydrogels

Previous studies have demonstrated red light-induced release of therapeutics from a B_{12} derivative that was conjugated with a drug molecule and a red light-capturing fluorophore at its upper axial ligand and ribose 5′-OH, respectively.[16] However, the synthesis of such B_{12} derivative is challenging and lacks generalizability.[9,15,17] We envisioned that the red-shifted $CarH_C$ variants could be used for the optically controlled release of proteins from materials scaffolds. To this end, we adopted a previously reported protein hydrogel system that comprised the assembly of the 4-arm star protein, $(SpyCatcher)_4$Snoop, and SpyTag-ELP-$CarH_C$-ELP-SpyTag (ACA).[8i] The two reactants were dissolved in a phosphate-buffered saline (PBS) containing the prelabeled Cy5-$CarH_C$-Ins164C (100 μM) and then mixed at a 1:2 molar ratio to form the molecular network through SpyTag/SpyCatcher chemistry. Subsequently, excess $AdoB_{12}$ (1.4 *eq.*) was added to immobilize Cy5-$CarH_C$-Ins164C onto the gel network via $CarH_C$ tetramerization (Figure 3A and 3B). The resulting gels were indeed sensitive to red light; on exposure to red light (~660 nm), the gels

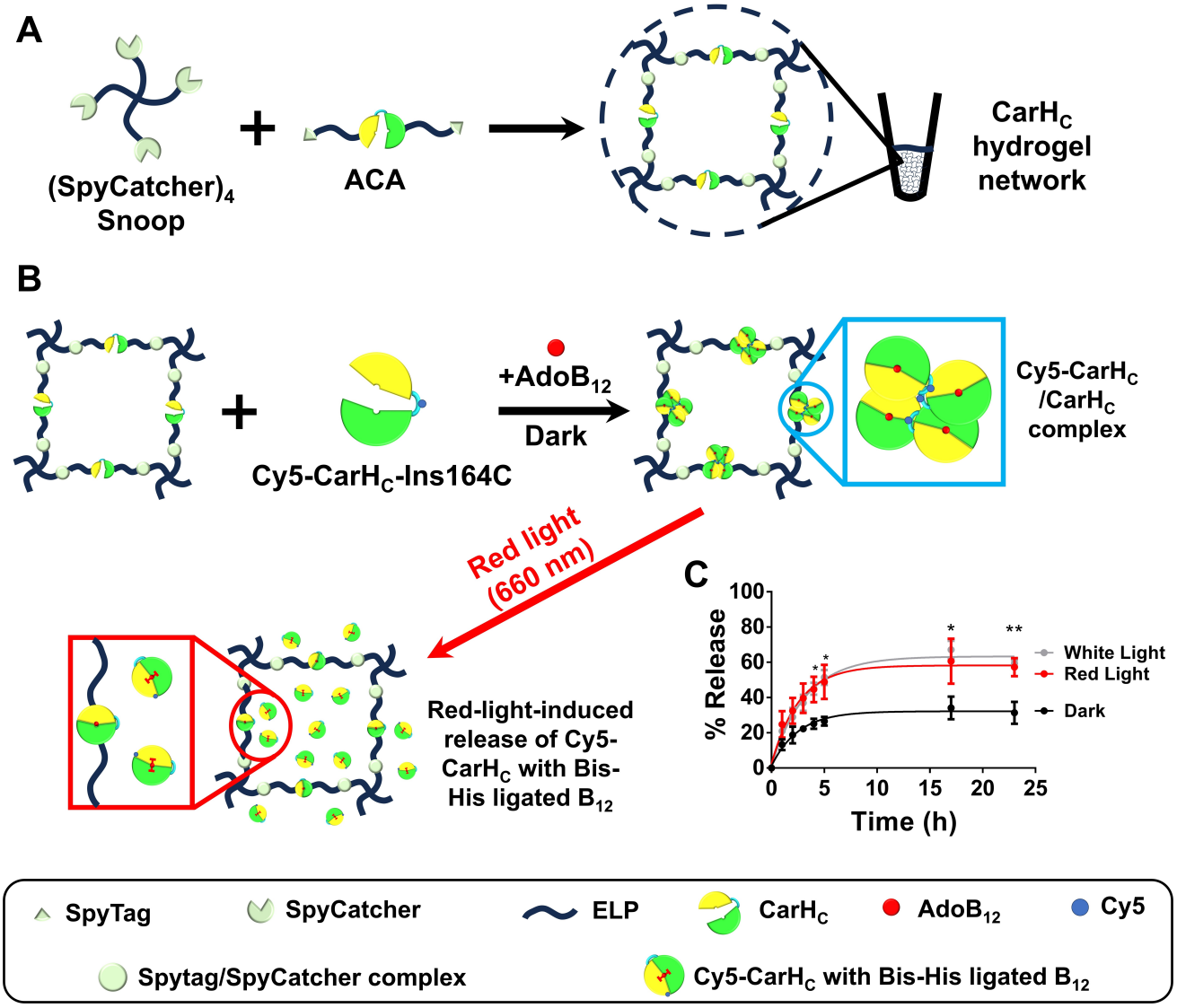

Figure 3. Fluorescent labeling enables red light-induced protein release from $CarH_C$ hydrogels. (A) Schematic showing the synthesis of protein hydrogels through the covalent assembly of the 4-arm star protein, $(SpyCatcher)_4$Snoop, and SpyTag-ELP-$CarH_C$-ELP-SpyTag (ACA) at a 1:2 molar ratio. (B) Schematic depicting $AdoB_{12}$-mediated immobilization of the prelabeled protein, Cy5-$CarH_C$-Ins164C, onto and subsequent red light-induced release from the protein hydrogel. (C) Release profile of Cy5-labeled $CarH_C$-Ins164C from $CarH_C$ hydrogels after red light (660 nm, 10 min, 0.1 mW/cm^2) or white light irradiation (10 min, 0.1 mW/cm^2). Data are presented as mean ± SD ($n=3$); a two-sided t-test was conducted at each time point, with p-values indicated as follows: * ≤ 0.05; ** ≤ 0.005. Data without asterisks indicate no significant differences ($p > 0.05$).

released up to 60 % of immobilized Cy5-CarH$_C$-Ins164C, as indicated by the fluorescence of Cy5 in the supernatant, which is comparable to those irradiated by white light (~60 %) and substantially higher than those kept in the dark (~28 %) (Figure 3C). To further confirm the role of Cy5-labeling in the red light-triggered release, we performed the control experiments with unlabeled CarH$_C$-Ins164C. The results showed that only ~20 % of CarH$_C$-Ins164C was released under red light, similar to those kept in the dark (Figure S16). This indicates that Cy5-labeling is necessary for the observed response of the gels to red light.

Admittedly, a considerable amount of proteins (~28 %) was released spontaneously even in the dark. This may reflect the combined contributions from incomplete cross-linking and the formation of ineffective loops, both of which are common in recombinant protein networks and thereby often account for passive gel erosion.[18] Loop formation can be more pronounced when reactions involve polymer precursors at millimolar concentrations, as shown in a previous study where loop fractions reached 80 % in networks formed from telechelic PEG oligomers at concentrations of approximately 5 mM.[19] On the other hand, the incomplete protein release (~60 %) after light exposure could be attributed to two possible factors. A considerable amount of photolyzed Cy5-CarH$_C$ remains weakly bound to the gel network, due to nonspecific hydrophobic effects. Additionally, the gel matrix itself may act as a diffusion barrier, trapping protein molecules within the hydrogel network.

Additionally, we have demonstrated optically controlled release of proteins from materials scaffolds in challenging deep tissue scenarios. Hydrogels immobilized with Cy5-CarH$_C$-Ins164C were subjected to to four conditions: (1) kept in the dark; (2) placed under pork meat and exposed to red light (660-nm LED, 0.5 mW/cm^2) for 10 minutes; (3) placed under pork meat and exposed to green light (520-nm LED, 0.5 mW/cm^2) for 10 minutes; (4) exposed to white light (Warsun®, 0.1 mW/cm^2) for 10 minutes. The results showed that up to 70 % of immobilized Cy5-CarH$_C$-Ins164C was released from the gels covered by pork meat upon exposure to red light or to white light, substantially higher than those beneath pork meat irradiated by green light (~30 %) or kept in the dark (~20 %), which clearly points to the advantage of the red-light responsive materials in a deep-tissue environment (Figure S17).

Together, these results showed that the red-shifted CarH$_C$ motif enables not only facile immobilization of proteins onto hydrogel scaffolds, but also controlled release in a red light-dependent manner in deep tissues.

Spectrally Tunable Protein Hydrogels Enabled by in situ Cy5 Labeling

Photoreceptor proteins such as UVR8, CarH$_C$, Dronpa145N, and Cph1, and PhyB/PIF6 have been used to create photoresponsive hydrogels, including those responsive to red/far-red light.[8a,d,e,i,j,20] However, the photoresponse of these gels is largely pre-determined by the photoreceptors and cannot be altered post-gelation. It would be desirable to have a hydrogel system, of which the photoresponse can be dynamically tuned in situ, independent of the material scaffold. Given the success of red-shifting CarH$_C$ via fluorescent labeling, we envisioned a way to create a photoresponsive hydrogel, spectrally tunable in situ, by incorporating cysteine-containing CarH$_C$ into the gel network. To achieve this, we chose (SpyCatcher)$_4$Snoop and AEC-G134C as the building blocks. The two precursors were mixed in a molar ratio of 1 : 4 to generate the four-arm star protein, (CarH$_C$-G134C)$_4$Snoop, followed by addition of 1.5 equiv. of AdoB$_{12}$ and 2 equiv. of Cy5-MAL, in relation to CarH$_C$-G134C, to initiate gelation and fluorescent labeling (Figure 4A). The rheological measurements in the time-sweep mode were used to monitor the gelation processes under different light conditions, including 1) initially exposed to red light (660 nm) for 2 hours and then kept in the dark, 2) those exposed to continuous white LED light, and 3) kept in the dark throughout the measurement. Although these reactions all led to the formation of elastic solid after ~9 h, with a steady $G' > G''$ revealed by frequency- and strain-sweep tests (Figure S18), light illumination significantly influenced the values of G' (Figure 4B, 4C and S18).The stiffness of the gels (G'~228.4 ± 94.2 Pa) after red light illumination was approximately 60 % of those formed in the dark or free of Cy5-MAL labeling (G'~388.6 ± 68.7 Pa) (Figure 4C). It is noteworthy that the Cy5-labeled gels formed under constant white light exhibited an even lower stiffness (G'~79.1 ± 34.6 Pa) compared to those under red light, indicative of a more thorough photolysis than under red light. However, despite the photolysis under white light, the G' value of the photodegraded products remained much higher than G'' (~10 Pa), suggesting possible chain entanglements among the protein polymers.

The discrepancy between the white light and red light conditions is likely attributed to the lower efficiency of in situ labeling utilized in the hydrogels (Figure 4). The in situ labeling efficiency was estimated with the changes of gel stiffness in response to red light and white light, $\Delta G'(\textit{red light}) / \Delta G'(\textit{white light})$, i.e., (388.6–228.4) Pa/(388.6–79.1) Pa ≈ 0.5, around 20 % lower than the pre-labeled proteins in Figure 2 (76 ± 2 %) (Figure S1), as determined by the UV/Vis absorbance spectra. In Figure 2C, the CarH$_C$ variants were pre-labeled with Cy5-MAL in significant excess (10 *equiv.*) to ensure optimal labeling efficiency. Any unreacted Cy5-MAL was subsequently removed by desalting before assessing their oligomerization states under light irradiation. Conversely, in Figure 4, Cy5-MAL (2 *equiv.*) was added to the gelation reaction mixtures, with the amount of Cy5-MAL limited by high protein concentrations; increasing the amount would lead to protein precipitation. As the proteins in the hydrogels were labeled with a much lower amount of Cy5-MAL in situ, making it seemingly less efficient than the pre-labeling method in Figure 2.

Nevertheless, these findings point to in situ fluorescent labeling of CarH$_C$ as a feasible approach to dynamically

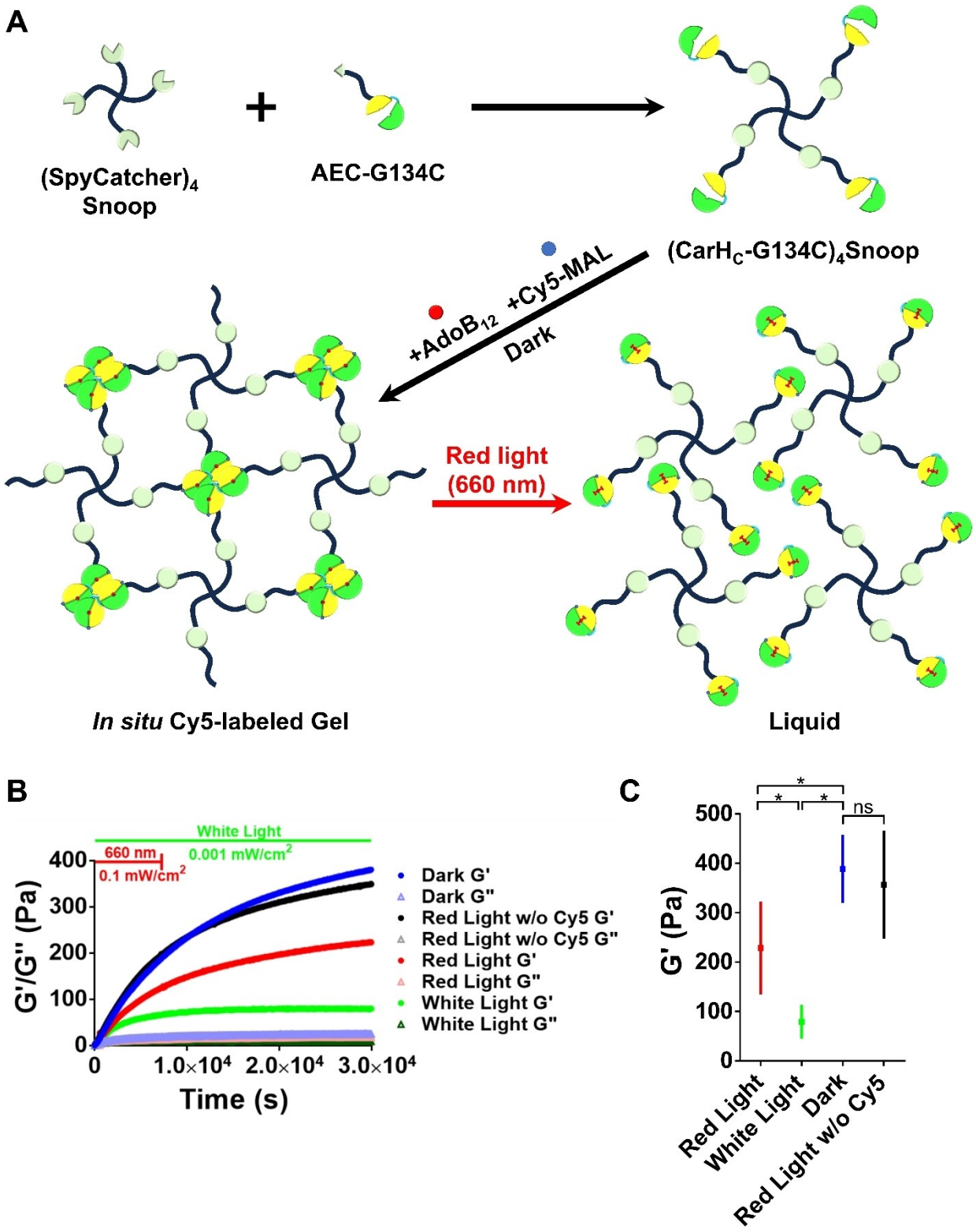

Figure 4. Red light induces erosion of $(CarH_C\text{-}G134C)_4$Snoop hydrogels in situ labeled with Cy5. (A) Schematic showing the synthesis of a red light-responsive hydrogel through the assembly of the 4-arm star protein, $(SpyCatcher)_4$Snoop, and SpyTag-ELP-$CarH_C$-G134C (AEC-G134C), with concurrent addition of $AdoB_{12}$ and Cy5-MAL. Exposure to red light disintegrates tetrameric Cy5-tagged $CarH_C$-G134C, leading to gel erosion. (B) Temporal evolution of storage modulus (G′) and loss modulus (G″) of in situ Cy5-labeled $CarH_C$ hydrogels under different irradiation conditions. (C) Final G′ values after erosion. Data are presented as mean ± SD ($n = 3$). A paired t-test was applied. $p^* \leq 0.05$; ns: no significance ($p > 0.05$). Red Light: red light irradiation for 2 h (660 nm, 0.1 mW/cm^2) followed by erosion in the dark; White Light: erosion under persistent ambient white light (0.001 mW/cm^2) throughout the measurement.

tune the photoresponse of protein materials, while circumventing complex molecular engineering efforts.

Reversible Cell-to-Cell Assembly/Disassembly Enabled by Cy5-CarH$_C$-G134C

The ability to precisely control the assembly (or disassembly) of living cells is crucial for designing tissue-like living materials with dynamic features.[21] In a previous study, we showcased the feasibility of using ultrahigh-affinity protein/protein interactions such as SpyTag/SpyCatcher and IM7/CL7 to assemble engineered *Saccharomyces cerevisiae* (baker's yeast) cells, a process that can be delicately controlled by microfluidics or optical tweezers.[21] However, the major interactions involved these multicellular assemblies are static and inert to external stimuli, necessitating alternative strategies for generating dynamically tunable, multicellular assemblies. Given the dynamic nature of CarH$_C$, i.e, AdoB$_{12}$-dependent tetramerization and green light-induced disassembly, we were prompted to explore the possibility of using CarH$_C$ and its red-shifted variants to create dynamic cell-to-cell assemblies that can sense and respond to external cues. To this end, we utilized the yeast cells that had previously been genetically engineered to express and display SpyCatcher.[21] Taking advantage of Spy chemistry, we first decorated the surface of yeast cells with AEC-G134C or its labeled counterpart Cy5-AEC-G134C; a pair of yeast cells were trapped by optical tweezers (1064 nm) and then immersed within the protein solution of AEC-G134C or Cy5-AEC-G134C in a microfluidic laminar flow chamber (Figure 5A, 5B and S19),[22] where far-red laser beams (1064 nm) were used to avoid interference with the photochemistry of Cy5 (~660 nm) and AdoB$_{12}$ (< 570 nm) in Cy5-AEC-G134C.

After decoration with Cy5-CarH$_C$-G134C, the optically trapped cells were then transferred to a channel filled with AdoB$_{12}$ and then brought into close contact by optical tweezers. We subsequently measured the adhesion forces between the cells by pulling them apart (Figure 5C). It turned out that the paired cells in the presence of AdoB$_{12}$ exhibited such strong adhesion that the force of up to 400 pN failed to separate them, in contrast to those in the absence of AdoB$_{12}$ that showed negligible adhesion forces. This dichotomy suggested that AdoB$_{12}$-induced CarH$_C$ tetramerization is essential for the strong intercellular interactions to form (Videos S2 and S3). The cell conjugates harboring the unlabeled CarH$_C$-G134C exhibited adhesion forces (447.7 ± 240.0 pN), comparable to those with the labeled Cy5-CarH$_C$-G134C, (481.0 ± 199.3 pN), suggesting that neither the mutation nor fluorescent labeling compromises the mechanical stability of CarH$_C$ tetramers. Moreover, these CarH$_C$-mediated intercellular interactions were comparable to those by SpyTag/SpyCatcher (334.6 ± 20.1 pN) and by CL7/Im7 (335.0 ± 48.7 pN), in spite of their respective covalent nature and ultrahigh affinity (K_d ~10^{-14} to ~10^{-17} M),[23] showcasing the exceptional mechanical stability of CarH$_C$ tetramers.

Nevertheless, fluorescent labeling made a difference in the photoresponse of these cell-to-cell interactions. For those cells harboring the unlabeled AEC-G134C, the intercellular adhesion force induced by AdoB$_{12}$ was significantly weakened (4.6 ± 2.2 pN) by green light, but remained largely unchanged (477.7 ± 105.5 pN) by red light, as expected for the photochemistry of CarH$_C$. On the other hand, the adhesion forces between the cells decorated with Cy5-CarH$_C$-G134C turned out to be sensitive to both green light (560 nm, 0.5 mW/cm^2, 2 min) and red light (660 nm, 0.5 mW/cm^2, 2 min, which were reduced from 481.0 ± 199.3 pN to 75.4 ± 143.4 pN and 32.3 ± 71.2 pN, respectively (Figure 5D). These irradiated cell conjugates were in effect disassembled, as the intercellular interactions after irradiation were comparable to those prior to addition of AdoB$_{12}$. Together, these results pointed to spectrally tunable CarH$_C$ as a viable motif for dynamic assembly and disassembly of living cells.

Spectral Tuning of Intercellular Interactions via in situ Fluorescent Labeling

The feasibility of using fluorescent labeling to spectrally tune CarH$_C$ in situ might add another dimension for regulating cell-to-cell interactions in living materials. To examine this, we genetically engineered yeast cells, rendering them to express and display AEC-G134C on the surface. A pair of cells were trapped using laser beams, subsequently moved to the channel filled with the solution containing both AdoB$_{12}$ and Cy5-MAL, and concurrently brought into proximity by the trapping laser beams (Figure 6A). In this process, AdoB$_{12}$ was responsible for eliciting the tetramerization of CarH$_C$ on the cell surface, and thus generating stable cell-to-cell conjugation, while Cy5-MAL was expected to react with Cys134 of AEC-G134C, thus red-shifting the photoresponse of the bicellular conjugates via optical coupling. To assess the influence of light on the resulting bicellular conjugates, we applied a persistent pulling force of ~200 pN to these conjugates under different illumination conditions. In the dark, these conjugates remained intact for an extended period (over 10 min), evidencing their marked mechanical stability (Figure 6B and 6C). In contrast, the conjugates were significantly destabilized both by red (660 nm) and green light (570 nm), corresponding to shortened duration of 127.5 ± 68.8 s and 197.9 ± 54.4 s, respectively (Figure 6B and 6C). The fact that the bicellular conjugates labeled by Cy5-MAL in situ gained a pronounced sensitivity towards red light, comparable to that toward green light, highlights the robustness of this optical coupling strategy in spectrally tuning B_{12}-dependent photoreceptors, even in a living system.

It is important to note that the in situ labeling with maleimide dyes, while intriguing, may not be suitable for certain in vivo applications due to the possible decoration of any free cysteine present. This limitation renders the technology more appropriate for ex vivo or in vitro applications, particularly those related to extracellular or cell-surface ligands or receptors.

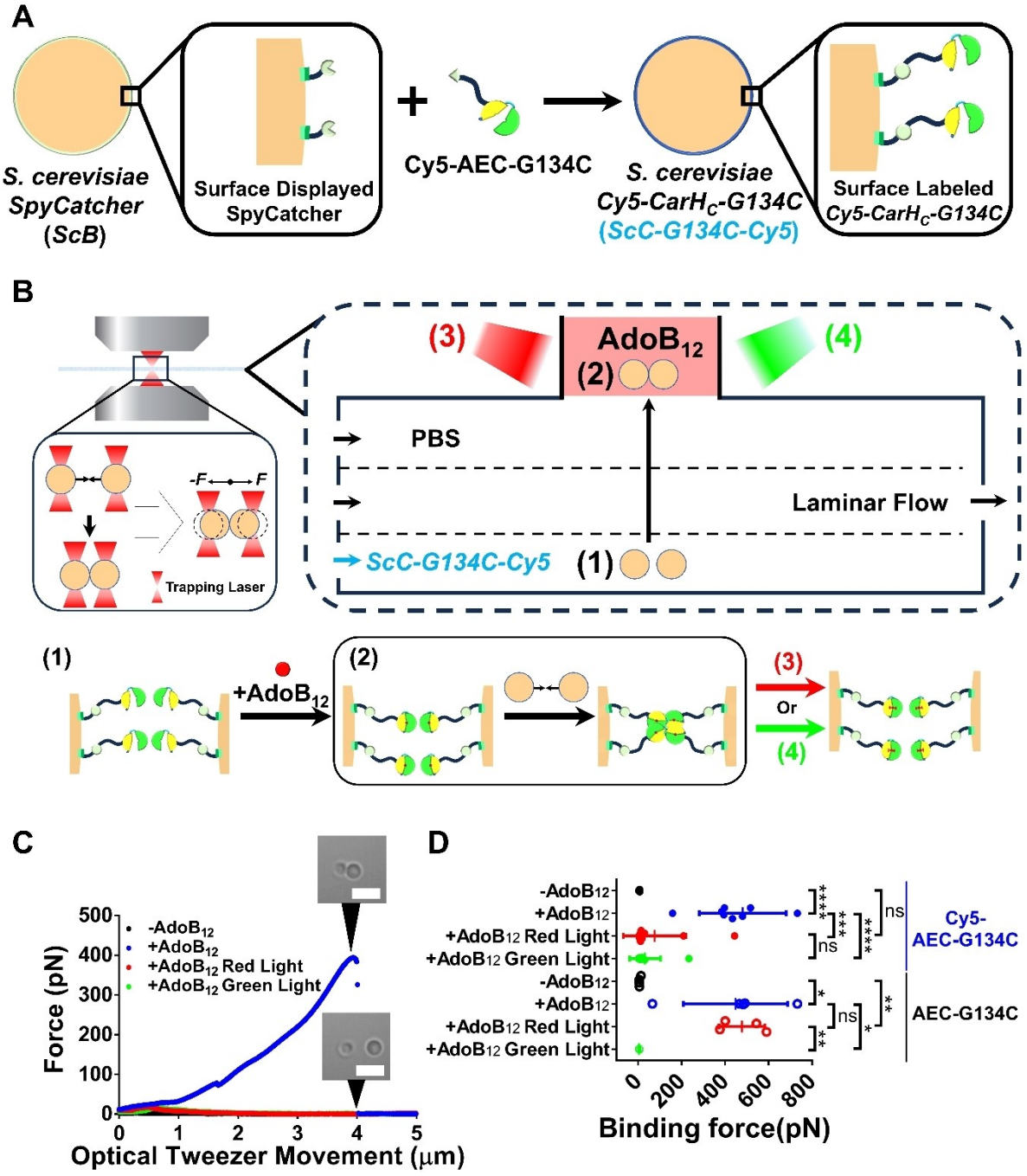

Figure 5. $CarH_C$ pre-labeled with Cy5 enables $AdoB_{12}$-dependent red light-responsive intercellular assembly. (A) Schematic showing decoration of SpyCatcher-displaying *Saccharomyces cerevisiae* cells with Cy5-tagged SpyTag-ELP-$CarH_C$-G134C (Cy5-AEC-G134C) through SpyTag/SpyCatcher chemistry. (B) Schematic illustration of assessing $AdoB_{12}$-induced intercellular conjugation and subsequent photo-induced dissociation using optical tweezers. The strength of intercellular conjugation was measured as the force required to tear apart the two cells during the following sequential operations: (1) trap two cells displaying Cy5-AEC-G134C, using trapping laser beams; (2) move the trapped cells to a chamber containing $AdoB_{12}$ and subsequently bring them into proximity to form cell-cell conjugation via $CarH_C$ tetramerization; (3 or 4) disassembling the paired cells by exposure to either red (3) or green light (4). (C) Binding forces between the paired cells during the three-step operations. The trapped cell was pulled away at a constant velocity (0.2 $\mu m\,s^{-1}$), and the measured force was recorded and plotted against movement distance. Representative force-distance graphs and snapshots depicting the trapped cells are shown. Scale bars, 5 μm. (D) Binding forces between the paired cells that display AEC-G134C with or without Cy5 labeling under various conditions. For the paired cells displaying Cy5-AEC-G134C: -$AdoB_{12}$, $n=9$; +$AdoB_{12}$, $n=9$; +$AdoB_{12}$ & red light (+$AdoB_{12}$ Red Light), $n=10$; +$AdoB_{12}$ & green light (+$AdoB_{12}$ Green Light), $n=10$. For the paired cells displaying unlabeled AEC-G134C: -$AdoB_{12}$, $n=4$. +$AdoB_{12}$, $n=5$. +$AdoB_{12}$ & RL, $n=4$. +$AdoB_{12}$ & GL, $n=5$. Data are presented as mean ± SD; Unpaired t-test was applied; p-values: **** ≤ 0.0001; *** ≤ 0.001; ** ≤ 0.01; * ≤ 0.05; ns: not significant (> 0.05).

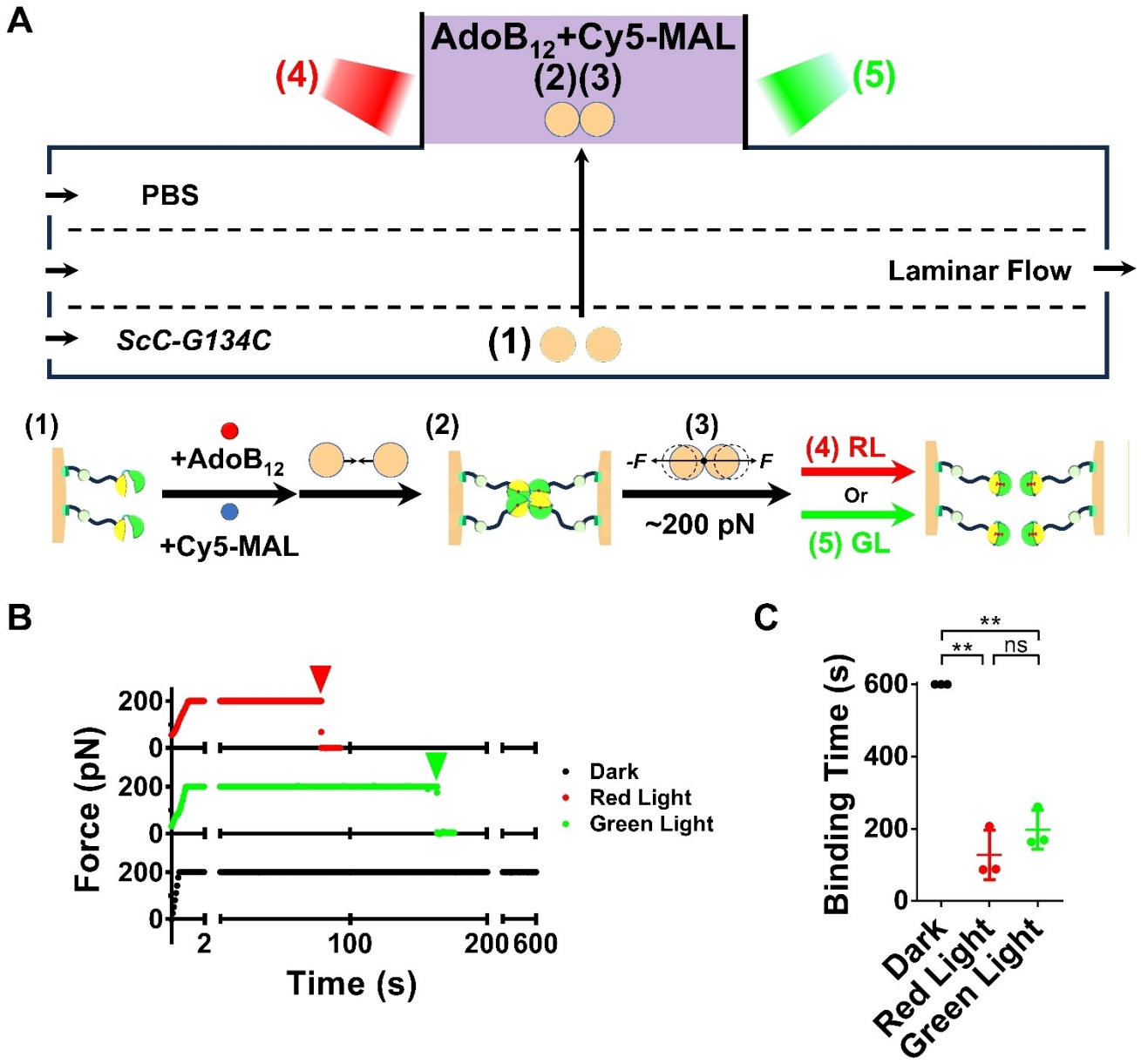

Figure 6. In situ Cy5 labeling enables red light-induced disassembly of cell-to-cell conjugates. (A) Schematic illustration of in situ Cy5-labeling of *Saccharomyces cerevisiae* cells that display SpyTag-ELP-CarH$_C$-G134C (AEC-G134C), AdoB$_{12}$-induced cell-to-cell conjugation, and subsequent photo-induced disassembly. Two AEC-G134C-displaying cells are trapped using the trapping laser beams (1), moved to a chamber filled with the solution containing both AdoB$_{12}$ (0.5 mM) and Cy5-MAL (0.5 mM), and subsequently brought into proximity to establish intercellular conjugation via CarH$_C$ tetramerization (2). Binding forces between the paired cells are measured before (3) and after irradiation of red light (4) or green light (5), using optical tweezers. (B) Influence of light irradiation on the duration of cell-to-cell conjugates under a persistent pulling force of ~200 pN. Representative force-time graphs are shown. Dark: no light exposure; Red Light: irradiated by red light (660 nm, 10 min, 0.5 mW/cm^2); Green Light: irradiated by green light (520 nm, 10 min, 0.1 mW/cm^2). Red and green triangles indicate the time point when cell pairs were torn apart under irradiation of red and green light, respectively. (C) Duration of cell assemblies under different irradiation conditions. Data are presented as mean ± SD ($n=3$); unpaired t-test was applied; p-value: ** ≤ 0.01; ns: not significant (> 0.05).

Conclusion

In summary, this study has demonstrated the feasibility of using optical coupling to red-shift B$_{12}$-dependent photoreceptor proteins; fluorescent labeling not only preserves the ability of CarH$_C$ to oligomerize upon the addition of AdoB$_{12}$ but also alters its subsequent photoresponse via contact quenching. This strategy presents two major advantages over the traditional spectral tuning methods based on protein engineering: 1) It streamlines the spectral tuning of optogenetic tools without the need for time-consuming trial-and-error processes often required in protein engineering. 2) It circumvents chemical modification of complex cofactors and avoids the potential perturbation of protein-cofactor interactions, thereby eliminating the need for additional protein engineering efforts. The resulting red-shifted photo-

receptors can be readily integrated into protein network and/or living cells, thus opening new avenues to dynamically tunable materials. This work represents a unique approach towards photoreceptor protein engineering and photoresponsive living materials, which holds great potential for future synthetic biology and optogenetics.

Acknowledgements

Funding support from Natural Science Foundation of China Excellent Young Scientists Fund 22122707 (F.S.); Ministry of Science and Technology 2020YFA0908100 (F.S.); GBA Institute of Collaborative Innovation GICI-001 (F.S.); Research Institute of Tsinghua, Pearl River Delta #RITPR-D21EG01 (F.S.); Shenzhen Science and Technology Innovation Committee/Shenzhen-Hong Kong-Macau S&T Program (Category C) SGDX2020110309460101 (F.S.); Research Grants Council of Hong Kong SAR GRF Grants #16103519 and #16103421 (F.S.), Research Fellow Scheme RFS2324-6S05 (F.S.), Young Collaborative Research Fund C6001-23Y (F.S.), Theme-based Research Scheme T13-602/21-N; Xin DAI acknowledges the funding support from "Laboratory for Synthetic Chemistry and Chemical Biology" under the Health@InnoHK Program launched by Innovation and Technology Commission, the Government of Hong Kong Special Administrative Region of the People's Republic of China.

Conflict of Interest

The authors declare no conflict of interest.

Data Availability Statement

Data available in article and on request

Keywords: cobalamin · material sciences · photoreceptor · protein engineering · protein modifications

[1] a) E. S. Boyden, F. Zhang, E. Bamberg, G. Nagel, K. Deisseroth, *Nat. Neurosci.* **2005**, *8*, 1263–1268; b) A. S. Chuong, M. L. Miri, V. Busskamp, G. A. C. Matthews, L. C. Acker, A. T. Sørensen, A. Young, N. C. Klapoetke, M. A. Henninger, S. B. Kodandaramaiah, M. Ogawa, S. B. Ramanlal, R. C. Bandler, B. D. Allen, C. R. Forest, B. Y. Chow, X. Han, Y. Lin, K. M. Tye, B. Roska, J. A. Cardin, E. S. Boyden, *Nat. Neurosci.* **2014**, *17*, 1123–1129.

[2] a) D. M. Palm, A. Agostini, S. Tenzer, B. M. Gloeckle, M. Werwie, D. Carbonera, H. Paulsen, *Biochemistry* **2017**, *56*, 1726–1736; b) M. Li, B. M. Park, X. Dai, Y. Xu, J. Huang, F. Sun, *Nat. Commun.* **2022**, *13*, 3197.

[3] a) S. Crosson, K. Moffat, *Proc. Natl. Acad. Sci. USA* **2001**, *98*, 2995–3000; b) L. Ma, Z. Guan, Q. Wang, X. Yan, J. Wang, Z. Wang, J. Cao, D. Zhang, X. Gong, P. Yin, *Nature Plants* **2020**, *6*, 1432–1438.

[4] a) R. J. Kutta, S. J. O. Hardman, L. O. Johannissen, B. Bellina, H. L. Messiha, J. M. Ortiz-Guerrero, M. Elías-Arnanz, S. Padmanabhan, P. Barran, N. S. Scrutton, A. R. Jones, *Nat. Commun.* **2015**, *6*, 7907–7907; b) X. X. Zhou, H. K. Chung, A. J. Lam, M. Z. Lin, *Science* **2012**, *338*, 810–814; c) J. Mailliet, G. Psakis, K. Feilke, V. Sineshchekov, L.-O. Essen, J. Hughes, *J. Mol. Biol.* **2011**, *413*, 115–127; d) W. Zhang, A. W. Lohman, Y. Zhuravlova, X. Lu, M. D. Wiens, H. Hoi, S. Yaganoglu, M. A. Mohr, E. N. Kitova, J. S. Klassen, P. Pantazis, R. J. Thompson, R. E. Campbell, *Nat. Methods* **2017**, *14*, 391–394; e) E. Burgie, A. Bussell, J. Walker, K. Dubiel, R. Vierstra, *Proc. Natl. Acad. Sci. USA* **2014**, *111*, 10179–10184; f) M. Oide, M. Nakasako, *Sci. Rep.* **2021**, *11*, 2827; g) G. I. Jenkins, *Curr. Opin. Struct. Biol.* **2014**, *29*, 52–57.

[5] a) C. N. Bedbrook, A. J. Rice, K. K. Yang, X. Ding, S. Chen, E. M. LeProust, V. Gradinaru, F. H. Arnold, *Proc. Natl. Acad. Sci. USA* **2017**, *114*, E2624–E2633; b) M. K. M. Engqvist, R. S. McIsaac, P. Dollinger, N. C. Flytzanis, M. Abrams, S. Schor, F. H. Arnold, *J. Mol. Biol.* **2015**, *427*, 205–220.

[6] a) S. Padmanabhan, M. Jost, C. L. Drennan, M. Elías-Arnanz, *Annu. Rev. Biochem.* **2017**, *86*, 485–514; b) M. C. Pérez-Marín, S. Padmanabhan, M. C. Polanco, F. J. Murillo, M. Elías-Arnanz, *Mol. Microbiol.* **2008**, *67*, 804–819; c) D. García-Moreno, C. Polanco María, G. Navarro-Avilés, J. Murillo Francisco, S. Padmanabhan, M. Elías-Arnanz, *J. Bacteriol.* **2009**, *191*, 3108–3119; d) M. Jost, J. Fernández-Zapata, M. C. Polanco, J. M. Ortiz-Guerrero, P. Y.-T. Chen, G. Kang, S. Padmanabhan, M. Elías-Arnanz, C. L. Drennan, *Nature* **2015**, *526*, 536–541.

[7] J. M. Ortiz-Guerrero, M. C. Polanco, F. J. Murillo, S. Padmanabhan, M. Elías-Arnanz, *Proc. Natl. Acad. Sci. USA* **2011**, *108*, 7565–7570.

[8] a) R. Wang, Z. Yang, J. Luo, I. M. Hsing, F. Sun, *Proc. Natl. Acad. Sci. USA* **2017**, *114*, 5912; b) S. Kainrath, M. Stadler, E. Reichhart, M. Distel, H. Janovjak, *Angew. Chem. Int. Ed.* **2017**, *56*, 4608–4611; c) C. Chatelle, R. Ochoa-Fernandez, R. Engesser, N. Schneider, H. M. Beyer, A. R. Jones, J. Timmer, M. D. Zurbriggen, W. Weber, *ACS Synth. Biol.* **2018**, *7*, 1349–1358; d) Z. Yang, Y. Yang, M. Wang, T. Wang, H. K. F. Fok, B. Jiang, W. Xiao, S. Kou, Y. Guo, Y. Yan, X. Deng, W.-B. Zhang, F. Sun, *Matter* **2020**, *2*, 233–249; e) B. Jiang, X. Liu, C. Yang, Z. Yang, J. Luo, S. Kou, K. Liu, F. Sun, *Sci. Adv.* **2020**, *6*, eabc4824; f) D. Xu, J. Ricken, S. V. Wegner, *Chem. Eur. J.* **2020**, *26*, 9859–9863; g) M. Mansouri, M.-D. Hussherr, T. Strittmatter, P. Buchmann, S. Xue, G. Camenisch, M. Fussenegger, *Nat. Commun.* **2021**, *12*, 3388; h) B. Nzigou Mombo, B. M. Bijonowski, S. Rasoulinejad, M. Mueller, S. V. Wegner, *Adv. Biol.* **2021**, *5*, 2000199; i) H. K. F. Fok, Z. Yang, B. Jiang, F. Sun, *Polym. Chem.* **2022**; j) Z. Yang, F. Fok Hong Kiu, J. Luo, Y. Yang, R. Wang, X. Huang, F. Sun, *Sci. Adv.* **2022**, *8*, eabm5482.

[9] T. A. Shell, J. R. Shell, Z. L. Rodgers, D. S. Lawrence, *Angew. Chem. Int. Ed.* **2014**, *53*, 875–878.

[10] a) R. B. Woodward, *Pure and Applied Chemistry* **1973**, *33*, 145–178; b) A. Eschenmoser, C. E. Wintner, *Science* **1977**, *196*, 1410–1420; c) I. E. Markó, *Science* **2001**, *294*, 1842–1843; d) K. ó Proinsias, M. Giedyk, D. Gryko, *Chem. Soc. Rev.* **2013**, *42*, 6605–6619; e) W. Craig, *J. Porphyrins Phthalocyanines* **2015**, *20*, 1550096.

[11] T. Schneider, Y. Tan, H. Li, J. S. Fisher, D. Zhang, *Comput. Struct. Biotechnol. J.* **2022**, *20*, 261–273.

[12] S. Zhang, L. N. Jeffreys, H. Poddar, Y. Yu, C. Liu, K. Patel, L. O. Johannissen, L. Zhu, M. J. Cliff, C. Yan, G. Schirò, M. Weik, M. Sakuma, C. W. Levy, D. Leys, D. J. Heyes, N. S. Scrutton, *Nat. Commun.* **2024**, *15*, 2740.

[13] a) J. Lee, Y. Choi, K. Kim, S. Hong, H.-Y. Park, T. Lee, G. J. Cheon, R. Song, *Bioconjugate Chem.* **2010**, *21*, 940–946; b) M. Ptaszek, *Prog. Mol. Biol. Transl. Sci.* **2013**, *113*, 59–108; c) B. K. Agrawalla, T. Wang, A. Riegger, M. P. Domogalla, K.

Steinbrink, T. Dörfler, X. Chen, F. Boldt, M. Lamla, J. Michaelis, S. L. Kuan, T. Weil, *Bioconjugate Chem.* **2018**, *29*, 29–34.
[14] W. Huang, X. Wu, X. Gao, Y. Yu, H. Lei, Z. Zhu, Y. Shi, Y. Chen, M. Qin, W. Wang, Y. Cao, *Nat. Chem.* **2019**, *11*, 310–319.
[15] a) C. C. Smeltzer, M. J. Cannon, P. R. Pinson, J. D. Munger, F. G. West, C. B. Grissom, *Org. Lett.* **2001**, *3*, 799–801; b) M. Lee, C. B. Grissom, *Org. Lett.* **2009**, *11*, 2499–2502.
[16] a) W. J. Smith, N. P. Oien, R. M. Hughes, C. M. Marvin, Z. L. Rodgers, J. Lee, D. S. Lawrence, *Angew. Chem. Int. Ed.* **2014**, *53*, 10945–10948; b) R. M. Hughes, C. M. Marvin, Z. L. Rodgers, S. Ding, N. P. Oien, W. J. Smith, D. S. Lawrence, *Angew. Chem. Int. Ed.* **2016**, *55*, 16080–16083; c) C. M. Marvin, S. Ding, R. E. White, N. Orlova, Q. Wang, E. M. Zywot, B. M. Vickerman, L. Harr, T. K. Tarrant, P. A. Dayton, D. S. Lawrence, *Small* **2019**, *15*, 1901442; d) L. N. Gendron, D. C. Zites, E. P. M. LaRochelle, J. R. Gunn, B. W. Pogue, T. A. Shell, J. R. Shell, *Photodiagn. Photodyn. Ther.* **2020**, *30*, 101637; e) B. M. Vickerman, C. P. O'Banion, X. Tan, D. S. Lawrence, *ACS Cent. Sci.* **2021**, *7*, 93–103; f) E. M. Zywot, N. Orlova, S. Ding, R. R. Rampersad, E. M. Rabjohns, V. A. Wickenheisser, Q. Wang, J. G. Welfare, L. Haar, A. M. Eudy, T. K. Tarrant, D. S. Lawrence, *Adv. Ther.* **2022**, *5*, 2100159.
[17] D. W. Jacobsen, in *Methods in Enzymology, Vol. 67*, Academic Press **1980**, pp. 12–19.
[18] F. Sun, W.-B. Zhang, A. Mahdavi, F. H. Arnold, D. A. Tirrell, *Proc. Natl. Acad. Sci. USA* **2014**, *111*, 11269–11274.
[19] H. Zhou, J. Woo, A. M. Cok, M. Wang, B. D. Olsen, J. A. Johnson, *Proc. Natl. Acad. Sci. USA* **2012**, *109*, 19119–19124.
[20] a) X. Zhang, C. Dong, W. Huang, H. Wang, L. Wang, D. Ding, H. Zhou, J. Long, T. Wang, Z. Yang, *Nanoscale* **2015**, *7*, 16666–16670; b) S. Lyu, J. Fang, T. Duan, L. Fu, J. Liu, H. Li, *Chem. Commun.* **2017**, *53*, 13375–13378; c) L. Liu, J. A. Shadish, C. K. Arakawa, K. Shi, J. Davis, C. A. DeForest, *Adv. Biosyst.* **2018**, *2*, 1800240; d) M. Hörner, K. Raute, B. Hummel, J. Madl, G. Creusen, O. Thomas, E. Christen, N. Hotz, R. Gübeli, R. Engesser, B. Rebmann, J. Lauer, B. Rolauffs, J. Timmer, W. Schamel, J. Pruszak, W. Römer, M. Zurbriggen, C. Friedrich, W. Weber, *Adv. Mater.* **2019**, *31*; e) J. A. Shadish, A. C. Strange, C. A. DeForest, *J. Am. Chem. Soc.* **2019**, *141*, 15619–15625; f) D. Xiang, X. Wu, W. Cao, B. Xue, M. Qin, Y. Cao, W. Wang, *Front. Chem.* **2020**, *8*; g) R. Emig, P. Hoess, H. Cai, P. Kohl, R. Peyronnet, W. Weber, M. Hörner, *Adv. Biol.* **2022**, *6*, 2000337; h) M. Hörner, J. Becker, R. Bohnert, M. Baños, C. Jerez-Longres, V. Mühlhäuser, D. Härrer, T. W. Wong, M. Meier, W. Weber, *Adv. Mater. Technol.* **2023**, *8*, 2300195.
[21] Q. Yi, X. Dai, B. M. Park, J. Gu, J. Luo, R. Wang, C. Yu, S. Kou, J. Huang, R. Lakerveld, F. Sun, *Sci. Adv.* **2022**, *8*, eade0073.
[22] N. Gera, M. Hussain, B. M. Rao, *Methods* **2013**, *60*, 15–26.
[23] a) B. Zakeri, J. O. Fierer, E. Celik, E. C. Chittock, U. Schwarz-Linek, V. T. Moy, M. Howarth, *Proc. Natl. Acad. Sci. USA* **2012**, *109*, E690–E697; b) M. N. Vassylyeva, S. Klyuyev, A. D. Vassylyev, H. Wesson, Z. Zhang, M. B. Renfrow, H. Wang, N. P. Higgins, L. T. Chow, D. G. Vassylyev, *Proc. Natl. Acad. Sci. USA* **2017**, *114*, E5138–E5147.

Manuscript received: June 12, 2024
Accepted manuscript online: September 6, 2024
Version of record online: November 6, 2024